

E36 experiment at J-PARC

Haiyun Lu, and Chaden Djalali for the E36 Collaboration
University of Iowa, Iowa City, IA 52242, USA
chaden-djalali@uiowa.edu

Abstract

The E36 experiment has been carried out at J-PARC to search for Lepton Universality violation in the kaon two body decays K_{l2} . A precise value of the decay width ratio $R_K = \Gamma(K_{e2}) = \Gamma(K_{\mu2})$ will be extracted and compared with the standard model (SM) value. Any sizable difference would suggest new physics beyond the SM. Simultaneously, E36 is sensitive to light U(1) gauge bosons which could be associated with dark matter or explain established muon-related anomalies (g-2). The experiment as well as the status of the analysis will be presented.

Key words: standard model; kaon detection; leptons; nonluminous matter; J-PARC; calibration; calorimeters; leptonic decay.

Experimento E36 en J-PARC

Resumen

El experimento E36 se ha llevado a cabo en J-PARC para buscar anomalías a la universalidad leptónica en las desintegraciones en dos leptones del kaón K_{l2} . Se extraerá un valor preciso de la fracción de anchos de desintegración $R_K = \Gamma(K_{e2}) = \Gamma(K_{\mu2})$ y se comparará con el valor del modelo estándar (SM). Cualquier diferencia considerable sugeriría una nueva física más allá del SM. Simultáneamente, E36 es sensible a los bosones de gauge ligeros U(1) que podrían estar asociados con la materia oscura o explicar anomalías relacionadas con el muón (g-2). El experimento y el estado del análisis serán presentados.

Palabras clave: modelo standard; detección de kaones; leptones; materia no luminosa; J-PARC; calibración; calorímetros; desintegración leptónica.

Introduction

The Standard Model (SM) has successfully explained the results of most particle and nuclear physics experiments [1]. However, it is believed to be just an effective low-energy description of fundamental interactions. The existence of dark matter and dark energy is completely beyond the scope of the SM, even though they make up most of the Universe. The fact that neutrinos have mass also cannot be explained by the SM. Therefore, the search for physics beyond the SM plays an important role in exploring the unknown areas of physics. The E36 experiment aimed to search for new physics beyond the SM mainly in terms of lepton universality violation. Furthermore, it also searches for dark photons possibly related to dark matter.

Recently the LHCb collaboration has made a measurement of the ratio of the branching ratio of the $B^+ \rightarrow K^+ \mu^+ \mu^-$ and $B^+ \rightarrow K^+ e^+ e^-$ decays to test μ - e universality. The value published was $0.745^{+0.90}_{-0.074}(\text{stat.}) \pm 0.036(\text{sys.})$ [2] for the dilepton invariant mass squared range $1 < q^2 < 6 \text{ GeV}^2/c^2$. The difference between this value and the SM prediction is about 2.6 standard deviations. The quantities $R_{D^{(*)}} = \frac{\mathcal{B}(B \rightarrow D^{(*)} \tau^+ \nu_\tau)}{\mathcal{B}(B \rightarrow D^{(*)} l^+ \nu_l)}$ where $l = \mu$ or e were measured [3, 4]

as $R_D^{\text{exp}} = 0.403 \pm 0.047$, $R_{D^*}^{\text{exp}} = 0.310 \pm 0.017$, which differs from the current Standard Model calculation [3] by 2.2σ and 3.3σ .

Materials, methods and results

1.1. K_{l2} decay and lepton Universality

Lepton universality is an assumption of the SM. Any violation of lepton universality is clearly a sign of new physics beyond the SM. Lepton universality states that the weak couplings of leptons are identical. A group of useful decays is the leptonic decays of pseudoscalar mesons. In the kaon sector, the decay width of $K^+ \rightarrow l^+ \nu_l(K_{l2})$, where l is μ^+ or e^+ , is

$$\Gamma(K_{l2}) = g^2_l \frac{G^2}{8\pi} f_k^2 m_k m_l^2 \left(1 - \frac{m_l^2}{m_k^2}\right)^2 \quad (1.1)$$

In E36, the decay width ratio of K_{e2} and $K_{\mu2}$

$$R_K = \frac{\Gamma(K_{e2})}{\Gamma(K_{\mu2})} = \left(\frac{g_e^2}{g_\mu^2}\right) \frac{m_e^2}{m_\mu^2} \left(\frac{m_k^2 - m_e^2}{m_k^2 - m_\mu^2}\right)^2 \quad (1.2)$$

is measured. R_K is free from the hadron decay constant and the sensitivity to new physics is enhanced by helicity suppression. In the SM, under the assumption of μ -e universality, the value is very precisely calculated [5],

$$R_K^{SM} = \frac{m_e^2}{m_\mu^2} \left((m_K^2 - m_e^2)(m_K^2 - m_\mu^2) \right)^2 (1 - \delta_\gamma) = (2.472 \pm 0.001) \times 10^{-5} \quad (1.3)$$

Here δ_γ is a correction due to the internal bremsstrahlung process (IB) which is also measured as K_{IV} in E36. The ratio providing a test of μ -e universality is

$$\frac{g_e}{g_\mu} = \left(\frac{R_K^{exp}}{R_K^{SM}} \right)^{\frac{1}{2}} \quad (1.4)$$

Any deviation of R_K^{exp} from R_K^{SM} is regarded as arising from the different coupling constants.

The Minimal Supersymmetric Standard Model (MSSM), which is the minimal extension to the SM that realizes supersymmetry with R parity is one candidate for new physics to be tested by R_K [6]. In the case of K_{l2} , a charged Higgs-mediated SUSY LFV contribution can be strongly enhanced by emitting a τ neutrino. This enhancement can possibly reach the percent level, $R_K^{LFV} = 1.013 R_K^{SM}$ [7, 8]. Recently a model with sterile neutrino mixing with inverse see-saw mechanism was also discussed [9].

The proton radius seems a completely different topic from lepton universality. However, the measurements of the proton radius used two leptons: muon and electron. The discrepancy between muonic and electronic measurements is 7 standard deviations [10, 11, 12, 13, 14]. Possible explanations are: violation of μ -e universality, strong-interaction effect entering in a loop diagram that is important for μp but not for $e p$, or the current published results are not as accurate as reported.

Search for dark photons

A dark photon is a $U(1)$ extension of the SM in the "dark" sector. The "dark" sector means that the particles do not interact with charges. However, the dark photon can mix with the normal photon with a parameter ε . In the simplest model, it couples weakly to the charge with strength εe [15]. This dark photon may explain the deviation in the g_μ -2 experimental measurement from the SM calculation. One can search for it by measuring all the charged decay particles and searching for a peak in the $e^+ e^-$ invariant mass spectrum. Our E36 apparatus can search for dark photons. The estimated yield of dark photon is at the order of 100 in the final states of $\pi^+ e^+ e^-$ and $\mu^+ \nu^+ e^+ e^-$ respectively by assuming $\varepsilon \sim 10^{-3}$ and about 10^{10} events of decaying kaons.

Experimental status of R_K

Recently, the KLOE and NA62 groups have published their results of R_K . The KLOE detector operated at DAΦNE, the Frascati $e^+ e^-$ collider system producing me-

sons. The number of collected events were 7064 ± 102 and 6750 ± 101 for K^+ and K^- in K_{e2} decay mode, respectively. The number of $K_{\mu 2}$ events was obtained from a fit to the missing mass squared m_1^2 distribution to be 2.878×10^8 for $K_{\mu 2}^+$ and 2.742×10^8 for $K_{\mu 2}^-$. The R_K value KLOE obtained was [16]

$$R_K = (2.493 \pm 0.025(\text{stat.}) \pm 0.019(\text{sys.})) \times 10^{-5} \quad (1.5)$$

This result quantitatively agrees with the SM prediction. The NA62 experiment at CERN collected a large sample of decays during a dedicated run in 2007-8 and their final goal was a measurement of R_K with 0.4% accuracy. Their beam line delivered K^+ and K^- beams in a narrow momentum band with a central momentum of 74 GeV/c. The momentum of the incoming kaon was not measured event-by-event, but instead, the averaged beam momentum was monitored using $K_{\pi 3}$ decays. With the narrow momentum spectrum, the K_{l2} decay was reconstructed by detecting a single track together with the missing mass technique. The number of K_{l2} candidates is $N(K_{e2}) = 59,803$ and $N(K_{\mu 2}) = 18.027 \times 10^6$. The result extracted by NA62 was [17]

$$R_K = (2.488 \pm 0.007(\text{stat.}) \pm 0.007(\text{sys.})) \times 10^{-5} \quad (1.6)$$

Experiment setup and status

A time-reversal experiment with kaons (TREK) was the original motivation for forming the collaboration. E06 [18] will be carried out at the extended Hadron Facility at the Japan Proton Accelerator Research Complex (J-PARC) in Japan. The E36 [19] experiment used many of the detector components proposed for E06, which are basically the E246 detectors [20, 21, 22]. The distinctive feature of the E36 experiment is utilizing a stopped kaon beam, which has quite different systematics from the previous in-flight experiments and is complementary to them.

The E36 experiment was carried out in the Hadron Hall at J-PARC in 2015. The area became available for installation in mid-November 2014 and the installation was completed in April 2015. The commission and test runs were performed in June. The commissioning data quality and the detector condition were checked during the summer. Several improvements were implemented including a trigger adjustment, and a new TTC (see figure 2) to improve the trigger efficiency. The production run was performed during October to December. The data acquisition (DAQ) was very stable during the whole experiment data-taking period with 10% dead-time at a trigger rate of 250 Hz [23].

J-PARC

J-PARC is an experimental facility with a set of high-intensity proton accelerators and several experimental sites utilizing the proton beam. It is open to users from around the world and located 150 km northeast of Tokyo. There are three proton accelerators: a 400 MeV linear accelerator, a 3 GeV rapid-cycling synchrotron (RCS) and a main ring synchrotron (MR) with 50 GeV

(currently 30 GeV). There are three experimental facilities using the proton beam: the materials and life science experimental facility (MLF), the hadron experimental facility, and the T2K experimental facility. Secondary beams are produced in the hadron facility and used for different experiments including E36.

Beam line

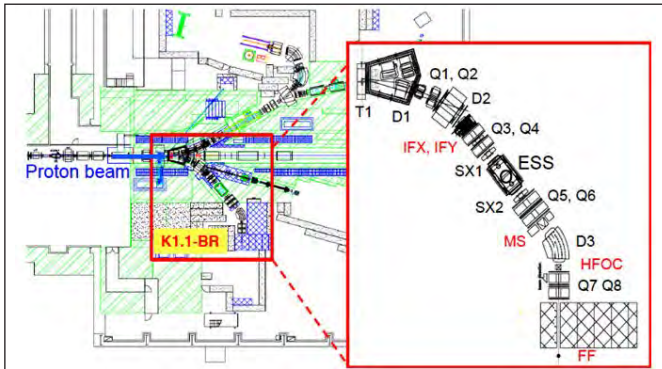


Figure 1. Layout of the K1.1BR beamline in the Hadron Facility of J-PARC

A secondary K^+ beam with momentum of 780 MeV/c was used and stopped in an active scintillating fiber target. As shown in figure 1, the beam line is about 20.3 m with three dipoles and eight quadrupole magnets. Although there is only one electro-static separator (ESS) and mass slit (MS), the vertical focus (IFY) before the ESS and the horizontal focus (HFOC) after the septum magnets play an important role to increase the K/π ratio. It was constructed in 2009 and commissioned in October 2010. A re-alignment was performed after the 2011 earthquake and it was re-commissioned in June 2012. A final K/π ratio of 1.0 has been achieved with 1.4×10^6 per spill at a proton intensity of 32 kW.

Overview of detector

A schematic side view of the detector is shown in figure 2. A Fitch Cherenkov counter is used to identify kaons and pions in the beam. The beam is slowed

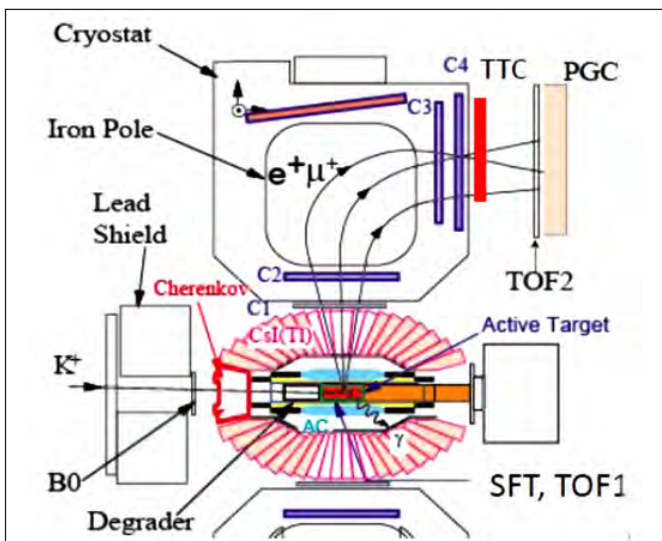


Figure 2. Schematic side view of the detector. The main components include a Fitch Cherenkov counter, an active target with SFT, a set of MWPCs, a CsI(Tl) system, two TOF systems, and a TTC.

down in a BeO degrader. An active target stops the beam and measures the decay vertex with the help of the spiral fiber tracker (SFT). An aerogel Cherenkov counter (AC), a Pb-glass counter (PGC) and a time-of-flight system (TOF1 and TOF2) identify electrons and muons. The spectrometer is composed of a superconducting toroidal magnet with 12 gaps, one multi-wire proportional chamber (MWPC) before each gap (C2) and two MWPCs rotated at 90 degrees after the gap (C3, C4). Radiative photons are detected by the CsI(Tl) calorimeter. A thin 3 mm trigger counter (TTC) was added after summer 2015. This increased the trigger purity with no hit position dependence.

Central detector

The active target downstream of the Fitch Cherenkov counter was a scintillator bundle made of 256 pieces of 3×3 mm² rectangular bars with a thin wavelength shifter (WLS) fiber embedded in a groove. The light through the WLS was read by a multi-pixel proportional counter (MPPC). To determine the coordinate of the kaon decay along the beam direction (z), a spiral fiber tracker (SFT) was added. Double-layer fiber ribbons with two helicities were wrapped around the target bundle. The effective length was about 200 mm. The detail of the winding was reported in [22]. The signals from the SFT and the

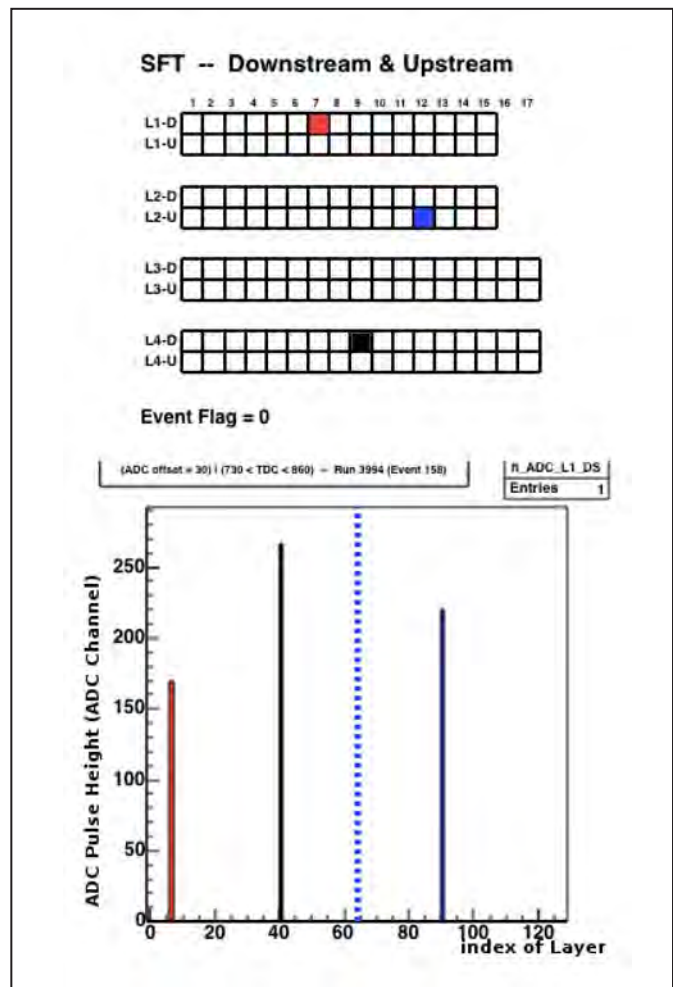


Figure 3. An example of SFT hits. Hit positions on different layers are shown on the left. The corresponding ADC values are shown on the right.

target provided complete vertex information. An example of SFT hits is shown in figure 3. The hits on different layers are shown on the left side and the corresponding ADC pulse heights on the right. An example event of target and TOF hits is shown in figure 4. The target fibers are labeled from 0 at the top left to 255 at the bottom right. The hits are colored to denote the ADC values. A stopping cluster is clearly seen together with a decay particle exiting at around Fiber 27. The hits in TOF1 and TOF2 are colored in green. They are consistent with the track at the target.

Spectrometer and particle identification

The central component of the spectrometer is a superconducting toroidal magnet with 12 iron sectors separated by 12 gaps. The target was placed in the center of the sectors. The superconducting magnet can generate a magnetic field up to 1.8 T. A field of 1.5 T was used for the production runs. $K_{\mu 2}$ muons from the center of the target are bent 90 degrees and tracked by C2 at the entrance, and C3 and C4 at the exit of the gap. The field map was calculated using the 3-dimensional code TOSCA and validated by measuring the monochromatic momentum spectra of $K_{\mu 2}$ and $K_{\pi 2}$.

To distinguish e^+ from μ^+ , an AC, a PGC and a pair of TOF1 and TOF2 scintillators were used. The thickness of the AC radiator was 4.0 cm and the refraction index of the aerogel material was 1.08. The e^+ detection efficiency is estimated to be greater than 98%. The PGC has a thickness of 12 cm with a radiation length $X_0=1.70$ cm. The e^+ efficiency was estimated about 98%. The misidentification probabilities of AC and PGC are typically 3% and 4%, respectively. TOF1 was located surrounding the target system and TOF2 was located about 90 cm behind C4 (see figure 2). A typical path length from TOF1 to TOF2 is 250 cm. The time resolution was about

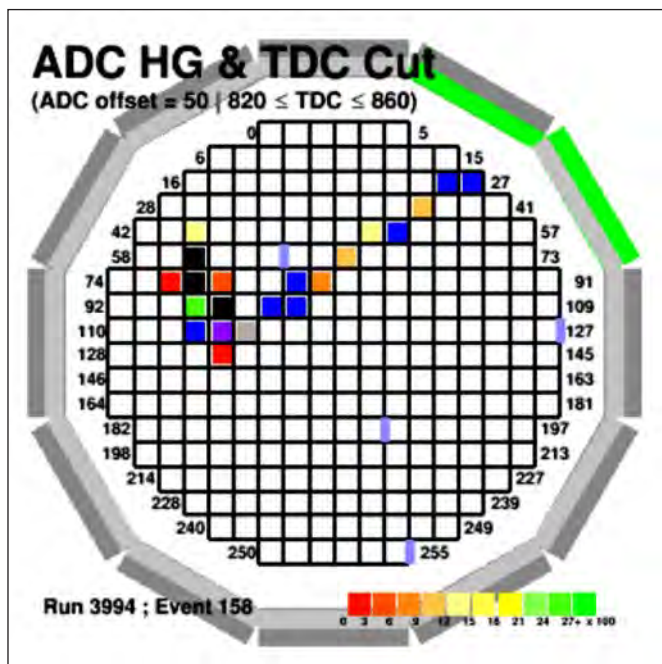


Figure 4. An event of target and TOF hits is displayed. The target fibers are labeled from 0 at the top left to 255 at the bottom right. TOF1 and TOF2 hits are shown in green.

200 ps. The time difference between the $K_{e 2}$ and $K_{\mu 2}$ events was approximately 500 ps. A small data sample is shown in figure 5. Analysis of AC and PGC is shown on the top as the momentum from the spectrometer versus ADC pulse height. The bottom left panel shows momentum versus the mass squared from the TOF analysis. After all the cuts are combined, the result is shown on bottom right, the bands of $K_{\mu 2}$ and $K_{e 3}$ clearly seen. The expected region of $K_{e 2}$ is indicated with red.

In the two-independent analysis scheme, the method of Kalman Filter is also being tried and tuned. Preliminary results showed the successful reconstruction of $K_{\mu 2}$ tracks.

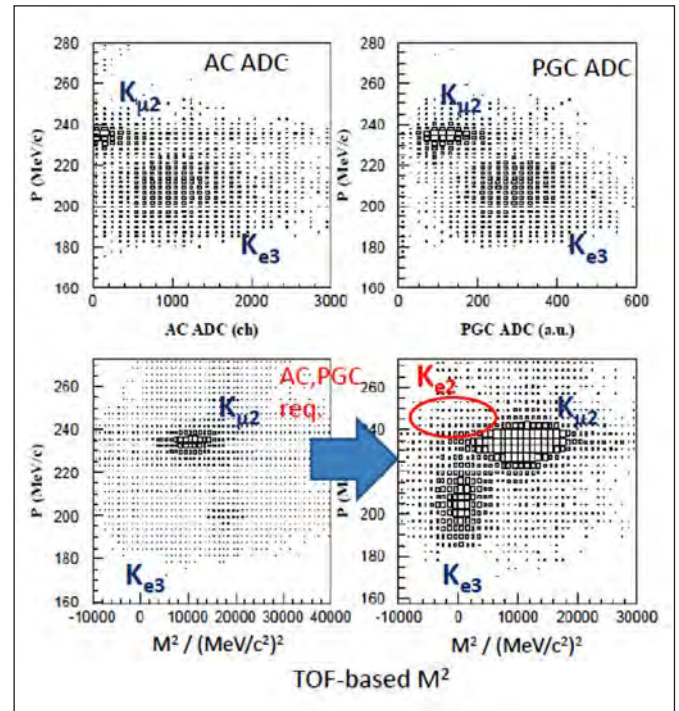


Figure 5. Example of PID analysis. Top left: AC ADC analysis (momentum vs. pulse height); top right: PGC ADC analysis; bottom left: TOF analysis; bottom right: all combined.

The CsI(Tl) calorimeter

The photon calorimeter was used to detect the radiative photons, for determining the disturbing structure dependent term, for the R_K measurement, as well as to detect the $e^+ e^-$ pair in the dark photon search. It consists of 768 CsI(Tl) crystals and covers 75% of the total solid angle. There are 12 holes for charged leptons and 2 holes for the beam entrance and exit. Twenty-four FADC modules were used to measure the amplified PIN diode signals from the CsI(Tl) crystals. Both hit time and energy deposited of each hit were extracted from the waveform digitized by FADCs, and the waveform can be used to decompose the signal pileup. The data was taken with cosmic rays when the beam was off to confirm the detector performance. The larger signal is interpreted as a stopped cosmic muon and the smaller pulse is the decay electron from the same muon. The distance between the two peaks is the decay time of the muon. The decay time of about 17,000 events were fitted and the extracted mean life time was $2.14 \pm 0.02 \mu\text{s}$.

Conclusion

The E36 collaboration has successfully completed data taking. Enough production, calibration and normalization data have been collected. The data quality has been checked with semi-online analysis. Off-line analysis is now underway. Offline calibration methods are being developed and implemented. Independent and collaborative efforts are distributed onto different tasks.

Reference

- [1] OLIVE KA, et. al. Review of Particle Physics. *Chin. Phys. C.* 2014; 38: 090001.
- [2] THE LHCb COLLABORATION. Test of Lepton Universality Using $B^+ \rightarrow K^+ l^+ l^-$ Decays. *Phys. Rev. Lett.* 2014; 113: 151601.
- [3] AMHIS Y, et. al. Averages of b -hadron, c -hadron, and τ -lepton properties as of summer 2016. *ArXiv:1612.07233*.
- [4] BERNLOCHNER FU, LIGETI Z, PAPUCCI M, ROBINSON DJ. Combined analysis of semileptonic B decays to D and D^* : $R(D^*)$, $|V_{cb}|$, and new physics. *Phys. Rev. D.* 2017; 95: 115008.
- [5] CIRIGLIANO V, ROSELL I. Two-Loop Effective Theory Analysis of $\pi(K) \rightarrow e\nu[\gamma]$ Branching Ratios. *Phys. Rev. Lett.* 2007; 99: 231801.
- [6] MASIERO A, PARADISI P, PETRONZIO R. Probing New Physics Through μ - e Universality in $K \rightarrow l\nu$. *Phys. Rev. D.* 2005; 74: 11701(R).
- [7] MASIERO A, PARADISI P, PETRONZIO R. Anatomy and Phenomenology of the Lepton Flavor Universality in SUSY Theories. *JHEP* 2008; 11: 011701
- [8] GIRRBACH J, NIERSTE U. $\Gamma(K \rightarrow e\nu)/\Gamma(K \rightarrow \mu\nu)$ in the Minimal Supersymmetric Standard Model. *JHEP.* 2010; 05: 026.
- [9] ABADA A, et. al. Tree-Level Lepton Universality Violation in the Presence of Sterile Neutrinos: Impact for R_K and R_{K^*} . *JHEP.* 2013; 02: 48.
- [10] SICK I. On the RMS-Radius of the Proton. *Phys. Lett. B.* 2003; 576: 62.
- [11] BERNAUER JC, et. al. High-precision determination of the electric and magnetic form factors of the proton. *Phys. Rev. Lett.* 2010; 105: 242001.
- [12] POHL R, et. al. The size of the proton. *Nature.* 2010; 466: 213.
- [13] MOHR PJ, TAYLOR BN, NEWELL DB. CODATA recommended values of the fundamental physical constants: 2010. *Rev. Mod. Phys.* 2012; 84: 1527.
- [14] ANTOGNINI A, et. al. Proton Structure from the measurement of 2S-2P transition frequencies of muonic hydrogen. *Science.* 2013; 339: 417.
- [15] ARKANI-HAMED N, et. al. A Theory of dark matter. *Phys. Rev. D.* 2009; 79: 015014.
- [16] The KLOE collaboration. Precise measurement of $\Gamma(K \rightarrow e\nu(\gamma))/\Gamma(K \rightarrow \mu\nu(\gamma))$ and study of $K \rightarrow e\nu\gamma$. *Eur. Phys. J. C.* 2009; 64: 627.
- [17] The NA62 collaboration. Precision measurement of the ratio of the charged kaon leptonic decay rates. *Phys. Lett. B.* 2013; 719: 326.
- [18] The TREK collaboration. The TREK experiment. Available in: <http://trek.kek.jp/trek.html>
- [19] The E36 collaboration. Precise measurement of $\Gamma(K^+ \rightarrow e^+\nu)/\Gamma(K^+ \rightarrow \mu^+\nu)$ using stopped positive kaons. Available in: <http://trek.kek.jp/e36/index.html>
- [20] ABE M, et. al. Search for T-violating transverse muon polarization in $K^+ \rightarrow \pi^0 \mu^+ \nu$ decay using stopped kaons. *Phys. Rev. Lett.* 1999; 83: 4253.
- [21] MACDONALD JA, et. al. Apparatus for A search for T violating muon polarization in stopped kaon decays. *Nucl. Instrum. Meth. A.* 2003; 506: 60.
- [22] DEMENTYEV DV, et. al. CsI(Tl) Photon detector with PIN photodiode readout for A $K_{\mu 3}$ T-violation experiment. *Nucl. Instrum. Meth. A.* 2000; 440: 151.
- [23] IGARASHI Y, LU HY, TANUMA R. Data acquisition system for the J-PARC E36 experiment. *IEEE-NPSS Real Time Conference* 2016. Available in: <http://ieeexplore.ieee.org/document/7543154/>
- [24] TABATA M, et. al. Assembly and bench testing of a spiral fiber tracker for the J-PARC TREK/E36 experiment. *JPS Conf. Proc.* 2015; 8: 024001.

Recibido: 13 de febrero de 2018

Aceptado: 29 de mayo de 2018